



Century-to-millennial scale climatic variability in Lake Malawi revealed by isotope records

Philip A. Barker^{a,*}, Melanie J. Leng^{b,c}, Françoise Gasse^d, Yongsong Huang^e

^a Department of Geography, Lancaster Environment Centre, Lancaster University, Lancaster LA1 4YQ, UK

^b NERC Isotope Geoscience Laboratory, British Geological Survey, Nottingham NG12 5GG, UK

^c School of Geography, University of Nottingham, Nottingham NG7 2RD, UK

^d CEREGE, UMR 6635, CNRS-Université Aix-Marseille III, 13545, Aix-en-Provence-cedex 04, France

^e Department of Geological Sciences, Brown University, Providence, Rhode Island, 02912, USA

Received 24 May 2006; received in revised form 7 May 2007; accepted 1 June 2007

Available online 12 June 2007

Editor: H. Elderfield

Abstract

Diatom-based oxygen isotope data ($\delta^{18}\text{O}_{\text{diatom}}$) from Lake Malawi show multi-centennial scale wet–dry intervals spaced approximately every 2.3 ka throughout a 25 ka sequence. The $\delta^{18}\text{O}_{\text{diatom}}$ record is supported by a lower resolution deuterium ($\delta\text{D}_{\text{pa}}$) isotope curve derived from palmitic acid. We interpret these isotope data in terms of major shifts in precipitation and evaporation moderated by seasonal controls on the host organisms. Dry periods marked by relatively positive isotope values, represent the extension of abrupt Holocene events noted from northern and equatorial Africa to 10–15°S. These events in Lake Malawi correspond to cool episodes in Greenland, thereby demonstrating teleconnections generated by meridional temperature gradients. Sea surface temperatures are likely to be the primary transmitter of deglacial climate changes, although trade wind strength and direction is critical in controlling precipitation patterns in tropical regions. Conversely, the global hydrological cycle, driven by low latitude regions represents an important positive feedback amplifying deglacial processes.

© 2007 Published by Elsevier B.V.

Keywords: isotopes; oxygen; diatoms; deuterium; palmitic acid; Malawi; palaeoclimate

1. Introduction

Energy excess in tropical regions dissipates latitudinally through atmospheric and oceanic circulation systems, at a rhythm partly controlled by the extent of polar ice sheets via meridional temperature gradients,

and the strength of the thermohaline circulation. Deciphering centennial-to-millennial scale variability in these bi-directional feedbacks is critical to understanding the relative roles of changing ocean and atmospheric circulation. In addition, zonal variability within the tropics, such as long periods of El Niño Southern Oscillation (ENSO)-like conditions (Stott et al., 2002; Rosenthal and Broccoli, 2004) can have extra tropical influence through perturbation of the global hydrological cycle (Chappellaz et al., 1993). The regional expression of these processes is complex, and

* Corresponding author. Department of Geography, Lancaster Environment Centre, Lancaster University, Lancaster LA1 4YB, UK. Tel.: +44 1524 593756; fax: +44 1524 847099.

E-mail address: p.barker@lancs.ac.uk (P.A. Barker).

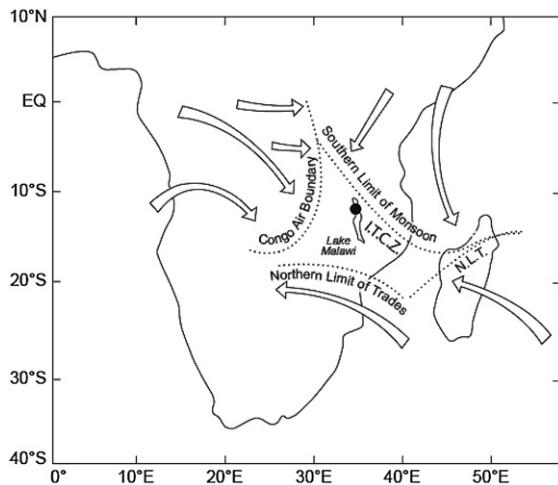


Fig. 1. Major surface airflow and convergence zones (dashed lines) influencing the Malawi region. The approximate position of the core site is marked with a black circle. Modified from (McHugh and Rogers, 2001).

our understanding is partial, since few sites preserve detailed records beginning before the last glacial maximum (LGM). Southern hemisphere localities are especially poorly represented in this climate mosaic, yet they are crucial to test phase relationships with polar regions as proposed by bipolar seesaw models (Broecker, 1998; Stocker, 1998). Here, these teleconnections are examined through a 25 ka diatom-based oxygen isotope record ($\delta^{18}\text{O}_{\text{diatom}}$) from the northern basin of Lake Malawi (10–15°S, 34.5°E), providing the first long continuous record of its kind from continental Africa. The $\delta^{18}\text{O}_{\text{diatom}}$ record is complemented by a lower resolution deuterium record from palmitic acid ($\delta\text{D}_{\text{pa}}$) and extends previous multiproxy palaeolimnological findings from the lake's northern basin (Barry et al., 2002; Gasse et al., 2002; Johnson et al., 2002; Filippi and Talbot, 2005).

1.1. Modern climate, hydrology and limnology

Lake Malawi's climate is largely controlled by the north–south migration of the inter-tropical convergence zone (ITCZ) that marks the meeting of the north-easterly monsoon and the south-easterly trade winds (Fig. 1). A north westerly airflow can also bring rain of Atlantic origin to Malawi via the Congo basin (McHugh and Rogers, 2001; Jury and Mwafulirwa, 2002). A single rainy season occurs during October–March when the ITCZ lies over the lake, and a dry season (April–September) is characterised by strong south-easterly trade winds. Mean rainfall over the catchment is

1350 mm yr⁻¹, but there is a steep north–south rainfall gradient due in part to the orographic influence of the northern Rungwe mountains. At the inter-annual scale, the Malawi catchment straddles the boundary between the southern subtropical and the equatorial climatic regions, which often respond to El Niño events by negative and positive annual rainfall anomalies, respectively (Nicholson, 1997). In general, Malawi receives greater or normal rainfall under La Niña conditions when the sea–land temperature gradient increases and convergence occurs over the continent, whereas in El Niño years the ascending limb of the Walker circulation moves eastward to the western Indian Ocean (Jury and Mpeta, 2004). Patterns of sea surface temperatures in the surrounding oceans are also important controls on the Rossby wave across southern Africa, bringing greater amounts of rain when the east Atlantic and Agulhas region are warm and the west Indian Ocean is relatively cool (Jury and Mwafulirwa, 2002). It has been demonstrated that under present boundary conditions higher rainfall south of 15°S occurs when Greenland is relatively cold and vice versa (Meehl and van Loon, 1979). Correlation with the North Atlantic Oscillation (NAO) and rainfall over the region helps define this process and implies that the ITCZ shifts southward when the NAO driven westerlies are strongest (McHugh and Rogers, 2001).

The climatology described above identifies ultimate source areas for Malawi rainfall as the western Indian

Table 1

Water isotope data from Lake Malawi collected at the end of the dry season 2002 from the southern basin

Location: Station D	Water depth (m)	$\delta^{18}\text{O}$	δD
Latitude/longitude 14.27° S 35.17° E December 2002	1	1.9	10.2
	5	1.9	10.3
	10	1.9	10.2
	20	1.9	8.9
	30	1.9	9.6
	40	2.0	n.d.
Senga Bay 13.75° S 34.62° E November 2002	0	2.0	9.7
	10	2.0	9.3
	20	1.9	10.0
	30	1.9	n.d.
	40	2.1	11.7
Senga Bay (2) 13.75° S 34.62° E December 2002	50	1.9	10.4
	0	1.9	10.5
	10	1.8	11.3
	20	1.9	11.5
	30	2.3	13.3
	40	1.9	12.6

No data: n.d. Units for $\delta^{18}\text{O}$ and δD are per mille (‰) compared to standard mean ocean water (SMOW).

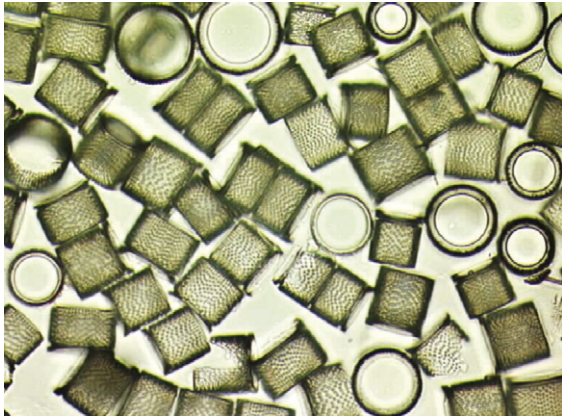


Fig. 2. A cleaned diatom sample from Lake Malawi comprised of *Aulacoseira nyassensis*.

Ocean and the tropical Atlantic. The importance of each source is not known and will change according to zonal circulation patterns such as ENSO and relative sea surface temperatures (SSTs) (Nicholson, 1997). Atlantic waters will become more isotopically enriched through recycling of transpired water from the Congo Basin as has been suggested from elsewhere in East Africa (Rozanski et al., 1996; Russell, 2004). The oxygen isotope composition of rainfall in the Lake Malawi catchment interpolated from the Global Network of Isotopes in Precipitation (GNIP) stations is -6 to -9‰ , with a marked ‘amount effect’ (higher rainfall intensity giving lower $\delta^{18}\text{O}$ and δD) during the wet season (IAEA/WMO, 1998). Deuterium values are similarly interpolated to be -14 to -38‰ . Direct precipitation and river discharge each represent $\sim 50\%$ of the water input to the lake, while evaporation and outflow contribute $\sim 84\%$ and $\sim 16\%$ of output, respectively (Ber-

gonzini, 1998; Bootsma et al., 2003) resulting in a net evaporative loss. Rivers north of 10.5°S discharge about 53% of total runoff. Water isotope values from the northern catchment are similar to rainfall estimates ($-3.1\text{‰} < \delta^{18}\text{O} < -5.4\text{‰}$ and $-14\text{‰} < \delta\text{D} < -31\text{‰}$) (Branchu et al., 2005). In contrast to these low rainfall and runoff values, we found the lake had high isotope values ($+1.8 < \delta^{18}\text{O} < +2.3\text{‰}$) measured at three stations from the southern basins to a depth of 50 m with only limited variation between measurements (Table 1). These values are comparable with deeper profiles from the central basin made in 1976 at the end of the wet season (Gonfiantini et al., 1979) and others from the northern basin at the end of the dry season in 1993 (Branchu et al., 2005). Our water isotope measurements were also made at the end of the dry season and represent maximum epilimnion values. Strongly enriched isotope values from the lake water, relative to those of the major inputs, testify to the fractionation exerted by evaporation from the lake surface.

Diatoms dominate the phytoplankton during the dry season when strong lake water mixing (April–September) (Hecky and Kling, 1987), low humidity and SE winds reinforce radiative cooling of surface water. All diatom silica is subject to some degree of dissolution during sinking and early diagenesis, but a rather high proportion (7 to 11%) of diatom production is permanently buried in Malawi (Bootsma et al., 2003). *Aulacoseira nyassensis* (Fig. 2) is the most ubiquitous diatom in cores from the northern basin and comprises the majority of the diatom biomass measured for $\delta^{18}\text{O}_{\text{diatom}}$. In addition to the diatom-based oxygen isotopes, we measured compound specific hydrogen isotope ratios as an alternative and complementary (to $\delta^{18}\text{O}_{\text{diatom}}$) insight into water isotope fractionation and palaeohydrology. It is important to note

Table 2
Chronology of core M98-2P based upon varve counts and radiocarbon results (Barry et al., 2002)

Depth (cm)	Calendar yr before 1998	^{14}C age (^{14}C yr BP)	2sigma maximum (cal yr BP)	Calibrated ^{14}C age intercepts (cal yr BP)	2sigma minimum (cal yr BP)	Laboratory code
5	323	–				(varve count)
35	552	–				(varve count)
53	698	–				(varve count)
139.5 B		2510 ± 50	2150	2000	1890	NOSAMS 18271
248.5 B		4020 ± 65	4080	3860	3690	NOSAMS 18272
379.5 B		6260 ± 65	6750	6640	6450	NOSAMS 18566
500.5 B		8820 ± 110	9500	9460, 9430	9030	NOSAMS 18692
537.5 B		9550 ± 120	10560	10230	9920	NOSAMS 18567
648.0 B		11450 ± 85	13160	13000	12680	NOSAMS 18561
744.0 C		14450 ± 100	17790	17360	16950	NOSAMS 18561
900.0 B		21000 ± 240		24170		NOSAMS 18693

Calibrated ^{14}C ages using Calib 4.2 (Stuiver et al., 1998), and a polynomial equation (Bard, 1998) for $21,000$ ^{14}C yr BP. A reservoir correction of 450 yr was subtracted before calibration. B = bulk sediment; C = Charcoal.

that the deuterium data are to be interpreted as a pilot study and full calibration of these data in tropical regions requires extensive further study.

2. Materials and methods

This study is based on core M98-2P core (9° 58.6' S, 34° 13.8' E, 363 m depth) from the northern basin of the lake collected by International Decade of East African lakes (IDEAL) programme members (Barry et al., 2002; Gasse et al., 2002; Johnson et al., 2002; Filippi and Talbot, 2005). Eight AMS radiocarbon analyses (Table 2) have been made on either total organic matter from M98-2P (seven dates) or charcoal (one date). The dates were found to be conformable to six previous dates on a nearby core (M98-1P) when correlated using ash marker horizons (Johnson et al., 2004). Core M98-2P contains sections of laminated sediments interspersed with homogeneous lake mud and five cm-scale ash horizons (Fig. 3). Detailed stratigraphical data is provided in earlier publications (Barry et al., 2002; Gasse et al., 2002; Johnson et al., 2002; Filippi and Talbot, 2005).

Core M98-2P was sampled at approximately 10 cm intervals for diatom-based oxygen isotope analysis, giving a mean resolution of 200 yr. Diatoms were

extracted using hot H₂O₂ and HNO₃, then sieved at 63, 38 and 20 µm and further concentrated using split cell thin flow (SPLITT) separation where necessary (Leng and Barker, 2006). For most samples the 63–38 µm or 38–20 µm fraction contained the majority of the diatom biomass. Our methodology successfully separated the diatoms from clays and volcanic ash. However, the cleaning process also removed small diatom taxa including most periphytic species and resulted in near monospecific samples dominated by *A. nyassensis* (Fig. 2). Although this skewed the diatom assemblage, it also eliminated any possible inter-specific variability in the acquisition of oxygen (Leng and Barker, 2006). A stepwise fluorination method was used to strip hydrous components from the diatom silica before a full reaction with BrF₅ (Leng and Barker, 2006). The oxygen liberated was then converted to CO₂ and normalised against NBS standards. Sample reproducibility was approximately 0.3‰.

Sediment samples for δD_{pa} were freeze-dried, and free lipids extracted using an Accelerated Solvent Extractor ASE200 using 2:1 (v/v) dichloromethane (DCM):methanol. Carboxylic acid fraction is isolated from the total extracts using solid phase extraction (Aminopropyl Bond Elute®), and was then methylated using anhydrous 2% HCl in Methanol. Methylated

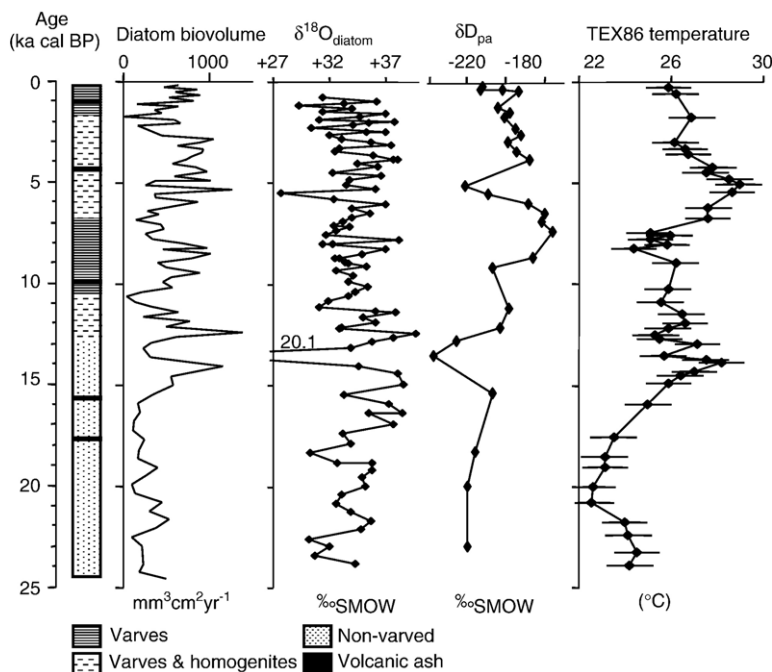


Fig. 3. Oxygen and deuterium isotope data from Lake Malawi core M98-2P. Diatom biovolume was calculated according to (Gasse et al., 2002). The TEX86 temperature curve is from (Powers et al., 2005).

carboxylic acid fractions were further purified using a silica gel flash column chromatography with DCM as the eluant (removes hydroxyl-carboxylic acids). Hydrogen isotope analyses were performed using a gas chromatography – high temperature conversion – isotope-ratio mass spectrometer (Huang et al., 2002). Compounds separated by GC column were converted to H_2 by a pyrolysis reactor at 1445 °C. Six pulses of hydrogen reference gas with known δD values were injected via the interface to the IRMS, for the computation of δD values of sample compounds. Typical standard deviation of triplicate analyses is $<\pm 2\%$. Internal standard heneicosane also showed consistent δD values throughout the analyses, with variability $<\pm 2\%$. The isotopic difference before and after derivatisation was used to calculate the δD value for the hydrogen from the added methyl group (Huang et al., 2002). δD values obtained from individual acids (as methyl esters) were corrected by mathematically removing the isotopic contributions from added groups before reporting.

Statistical treatment of the $\delta^{18}O_{\text{diatom}}$ data used Analyseries v.1.2 (Paillard et al., 1996). Singular spectrum analysis (SSA) was applied to enhance the signal/noise ratio and to highlight the periodicities evident in the raw diatom record (embedding dimension: 20; Vautard–Ghil autocovariance estimation) (Ghil et al., 2002). Data were re-sampled every 200 yr, normalised by their standard deviation and detrended for their long-term linear trend before performing the SSA. Periodograms of the raw data and SSA filtered data were performed using the Blackman–Tukey method (analysis of 50% of the series; Bartlett window).

3. Results and interpretation

The Malawi diatom-based oxygen isotope values span a range of 18‰ (Fig. 3). A part of this range is accounted for by lake water temperature as values of $\delta^{18}O_{\text{diatom}}$ are governed by both temperature and the isotope composition of lake water (a function of source water, precipitation and evaporation) at the time the diatom frustules formed. Temperature has been estimated independently from these cores using the TEX₈₆ index (the average number of cyclopentane rings incorporated into membrane lipids of Crenarchaeota) (Powers et al., 2005), and suggest surface temperatures compared to modern values (25–29 °C) of –3.5 °C during the LGM, –1 °C during the YD and around 8.2 ka BP, and values of +3 °C and +5 °C were calculated for ca. 13.8 ka and 5 ka BP (Fig. 3). Temperature changes of this order and published $\delta^{18}O_{\text{diatom}}$ fractionation factors

of –0.2 to –0.5‰ per °C (Juillet-Leclerc and Labeyrie, 1987; Shemesh et al., 1992) do not alter significantly the $\delta^{18}O_{\text{diatom}}$ curve. Instead, the variation in $\delta^{18}O_{\text{diatom}}$ must derive mainly from changes in the Lake Malawi water isotope composition ($\delta^{18}O_{\text{lake}}$), itself a function of precipitation (amount and source), temperature, and evaporation. A sensitivity analysis of lake waters to changes in climate parameters (Ricketts, 1998) has showed that a 1‰ depletion in $\delta^{18}O_{\text{lake}}$ would need either a 3.7 °C decrease in temperature, a 6.7 mS^{-1} increase in windiness, a 17% decrease in humidity, or a 1.4‰ depletion in $\delta^{18}O$ of inputs. Since evaporation enriches the lake by 8‰ relative to precipitation at the present day, large changes in water isotope values in the past will have resulted from shifts in precipitation–evaporation (P–E). Understanding of the acquisition of $\delta^{18}O_{\text{diatom}}$ values by diatoms has increased significantly but no study of a large lake has yet been able to make a fully quantitative reconstruction of lake water isotope hydrology analogous to that achievable from calcite (Leng and Barker, 2006). A major source of uncertainty is the early diagenetic alteration of frustules post mortem (Schmidt et al., 2001) that can cause an offset between lake water isotope conditions and that recorded by sedimentary diatoms. There is very little evidence of dissolution in these sediments although maturation processes causing infilling of pore spaces within the frustule cannot be discounted. In the absence of a detailed modern sampling programme, relating seasonal $\delta^{18}O_{\text{diatom}}$ values from plankton tows to sediment trap and surface sediments, that is beyond the scope of this present study, our interpretation is limited to relative changes in $\delta^{18}O_{\text{diatom}}$.

Support for the predominance of water balance considerations in the interpretation of $\delta^{18}O_{\text{diatom}}$ comes from a correlation between diatom biovolume, a surrogate for diatom productivity and $\delta^{18}O_{\text{diatom}}$. Singular spectrum analysis (Ghil et al., 2002) reveals the underlying variability in these curves and a positive linear correlation between the two filtered time series ($r^2=0.63$) for the last 15 ka. Diatom productivity is greatest during the dry season today and during decadal-scale low lake level stages within the past 200 yr (Gasse, unpublished data). Before 15 ka the relationship decouples, as other factors such as external loadings of Si and P, nutrients essential to diatom productivity, would have become limiting under generally dry glacial conditions (Bootsma et al., 2003; Johnson et al., 2004).

Good agreement is found between the $\delta^{18}O_{\text{diatom}}$ and δD_{pa} values (Fig. 3). This is expected since lake water provides the source of both the diatom oxygen and the deuterium within palmitic acid (an aliphatic carboxylic

acid that reacts with glycerol to form lipids in a broad range of organisms) providing that the lipids extracted from the sediments are of aquatic origin. The source of the organic material is important since higher plants can be enriched in δD by 10–60‰ relative to aquatic tissues due to direct use of meteoric waters and physiological factors (Sachse et al., 2004). A correlation with lake water isotope values and measured δD from palmitic acid contained in lake sediments across North America has been established (Huang et al., 2002), but in a large complex lake such as Malawi, this assumption requires further testing. The organic matter in these deepwater Lake Malawi sediments is largely of algal origin as demonstrated by C/N, $\delta^{13}C$, $\delta^{15}N$ and HI values, although the relative contribution of terrestrial and aquatic sources is variable (Filippi and Talbot, 2005).

Our interpretation of the two diatom and palmitic acid isotope curves is therefore broadly similar, yet some differences can be anticipated according to the processes of isotope acquisition, the provenance of the palmitic acid and seasonal differences between the isotope hosts. Seasonality in lake water isotope values is important since diatom productivity is skewed toward the cooler, windier dry season. Like the bulk organic matter, the aquatic lipids contain a significant algal component derived from a weighted sum of all three major groups; namely Cyanobacteria, Chlorophytes and diatoms, found in the lake in varying ratios during the annual cycle (Bootsma, 1993). Whereas the diatoms will incorporate a dry season isotope signature, if the palmitic acid was largely from other algae, a greater proportion of the deuterium would be incorporated during the strongly stratified wet season. Inter-annual variation between algal groups and the amount of biomass they produce will have occurred throughout this 25 ka series, leading to differences in the season represented by the deuterium isotopes. The oxygen and deuterium isotope curves are likely to diverge most strongly when diatom productivity is low relative to that of the lake as a whole, as probably occurred during the LGM when Si limited diatom production (Johnson et al., 2002), or if high runoff brought more abundant higher plant material to the deep waters.

3.1. The pre-Holocene period

A general pattern of increasing $\delta^{18}O_{\text{diatom}}$ values, punctuated by a series of wet–dry fluctuations, can be observed from the core base to ca. 15 ka, when following a major wet period, oxygen isotope values oscillate at centennial to millennial scales around the mean of the record. Given the range of indicators which

suggest evidence for relative aridity at the LGM and a lower lake level (Gasse et al., 2002; Johnson et al., 2002; Barker and Gasse, 2003; Filippi and Talbot, 2005), it is perhaps surprising that both of the isotope curves do not contain values that are more enriched in the heavier isotope. One explanation of relative high values of δD_{pa} is that the majority of autochthonous production at this time derived from Cyanobacteria and Chlorophytes using nutrients delivered during a shortened wet season or from upwelling. Low diatom biovolume and biogenic silica flux (Johnson et al., 2002) indicates only weak diatom growth occurred around the LGM, probably due to silica becoming rapidly limited if catchment inputs of silica were reduced under a drier climate (Fig. 3), and a switch toward other algal groups would have been likely.

Specific wet-dry periods in the $\delta^{18}O_{\text{diatom}}$ record can be correlated with proxies from neighbouring sites, including the relatively wet interval 17–18 ka that can be found in lake Tanganyika to the north and in the Makapansgat stalagmite oxygen isotope record from South Africa (Holmgren et al., 2003). More generally, the millennial scale variability in the $\delta^{18}O_{\text{diatom}}$ record corresponds to temperature changes at high latitudes, although broadly opposing relationships are observed with Greenland (GISP2; Grootes et al., 1993) and during the postglacial period with Antarctica (eg. Dronning Maud Land (Oerter et al., 2004)) (Fig. 4). According to these data, centennial-scale dry periods in Malawi occur when Greenland is relatively cold (Brook et al., 2005), and vice versa. For example, dry events ca. 21.5–22 ka and 19–20 ka coincide with cool periods in the GISP2 temperature reconstruction. Moreover, the most extensive dry period in our record from 17.8–14.5 ka corresponds to the cool interval preceding the Bølling–Allerød (BA) in Greenland and the major postglacial warming of Antarctica. The highest $\delta^{18}O_{\text{diatom}}$ value (+39.7‰), representing the most intense dry period in this sequence is recorded at 12.5 ka, the start of the exceptionally cold Younger Dryas in Greenland. Conditions at lake Malawi during the Younger Dryas are complex and show a second maximum dry phase at 11.8 ka before the establishment of wet Early Holocene conditions. Relatively high concentrations of periphytic diatoms, a diminished silica flux to the lake and organic matter composition support the interpretation that these were relatively dry periods (Gasse et al., 2002; Johnson et al., 2004; Filippi and Talbot, 2005). Other data from this core show low P, suggesting reduced river inputs, and variable volcanic ash inputs brought either by northerly wind or rivers to the lake from the northern catchment during many of the dry intervals described

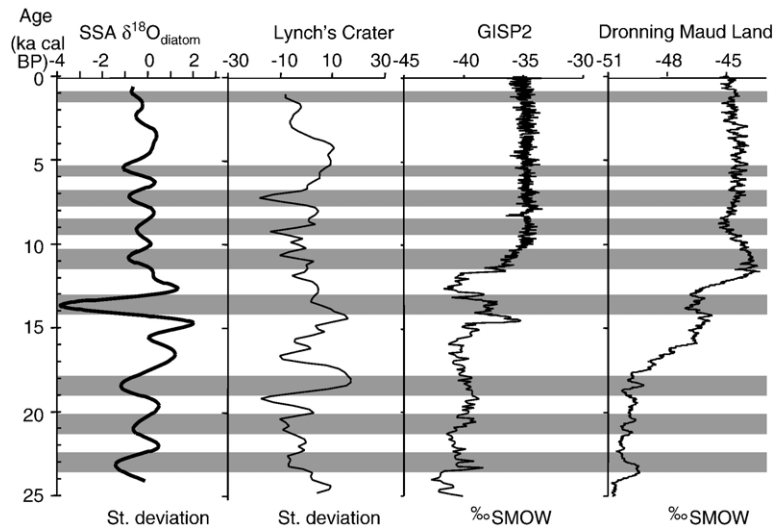


Fig. 4. Comparison of SSA smoothed $\delta^{18}\text{O}_{\text{diatom}}$ curve, with a peat humification series from Lynch's Crater, Australia (illustrated here by the smoothed detrended % absorption series) (Turney et al., 2004), GISP2 $\delta^{18}\text{O}$ (Grootes et al., 1993) and Dronning Maud land, Antarctica $\delta^{18}\text{O}$ (Oerter et al., 2004). The SSA of $\delta^{18}\text{O}_{\text{diatom}}$ is based on the first 6 principal components accounting for 68% of the explained variance. The Lynch's Crater record is detrended and smoothed using a 3 point Gaussian filter (Oerter et al., 2004). Grey bands represent relatively wet periods in lake Malawi.

here (Johnson et al., 2002). The organic matter record shows high primary productivity from 17.9–16.5 ka and has been interpreted as indicative of high nutrient flux from increased runoff (Filippi and Talbot, 2005). But, diatom productivity was low at this time, suggesting that at least the supply of Si did not increase, and instead it could be envisaged that stronger vertical mixing led to more efficient regeneration of N in the epilimnion, thereby shifting lake water stoichiometry and altering competitive interactions amongst phytoplankton in favour of Cyanobacteria.

Around 13.5 ka there is a remarkable decrease in $\delta^{18}\text{O}_{\text{diatom}}$ coeval with a minimum in diatom periphyton (Gasse et al., 2002). This negative oxygen isotope spike has been replicated and corresponds to a similar excursion in the $\delta\text{D}_{\text{pa}}$ data and corresponds to a peak in water temperature inferred from TEX_{86} (Powers et al., 2005). These independent measurements indicate that these unusual values had a physical underpinning and cannot be dismissed as experimental error. The correspondence with $\delta\text{D}_{\text{pa}}$ suggests that isotopic dilution was brought about by an increase in rainfall over the catchment, and the lake reaching its overflow after several millennia of closure may have amplified the response. This remarkable wet phase in the Malawi basin occurred during the Antarctic Cold reversal (Jouzel et al., 1995) and the second half of the warm BA period in Greenland. It falls within the major postglacial expansion of more northerly lakes that began ca. 15 ka in Tanganyika (Gasse et al., 1989),

Victoria (Johnson, 1996), Rukwa (Haberyan, 1987; Barker et al., 2002), Manyara (Holdship, 1976), Magadi (Roberts et al., 1993) and others (Barker and Gasse, 2003), although these proxy (mainly diatom) records show a protracted wet period until at least the Younger Dryas.

3.2. The Holocene

The Early and Middle Holocene reveals a series of wet–dry fluctuations around the mean values for the sequence and is relatively stable compared to earlier and succeeding periods (Figs. 3 and 4). The record suggests relatively high P–E at ca. 11.0, 9, 7.5 ka and maximum aridity at 10, 8.2, and 6.4 ka. Relatively dry conditions at 8.2 ka are well known from several high resolution sites in East Africa (Barker et al., 2004). Around 7 ka we observe some minor differences between the shape of the $\delta\text{D}_{\text{pa}}$ and that of the $\delta^{18}\text{O}_{\text{diatom}}$ curve. Seasonal differences in the acquisition of water isotopes could again have occurred as proposed for earlier parts of the record, although contamination with higher plant material would offer a simpler explanation to high $\delta\text{D}_{\text{pa}}$, especially as inputs of terrestrial remains from the lake margin are suggested by the organic matter composition (Filippi and Talbot, 2005). The period ends with a wet pulse at 5.3 ka confirmed by a sharp peak in $\delta\text{D}_{\text{pa}}$ and coeval with the warmest lake water temperatures (Powers et al., 2005). After 5 ka, the frequency of changes increases, but the underlying trend

indicates relative aridity around 4 ka followed by a return to values around the mean of the series.

4. Palaeoclimatic implications

Millennial–centennial scale fluctuations in the Lake Malawi $\delta^{18}\text{O}_{\text{diatom}}$ values are inversely related to Greenland temperatures during the deglaciation as measured by the GISP2 temperature record (Grootes et al., 1993). Relationships with Antarctica are less clear since the stadial–interstadial pattern is weaker during the deglaciation, although some suggestion of an opposing or lagged response to ice core temperatures (Blunier and Brook, 2001) can be observed, in accordance with the bipolar seesaw hypothesis (Broecker, 1998). Positive fluctuations of the large northern ice sheets and to a lesser extent Antarctic sea ice, increased meridional temperature gradients, sucked heat from the tropics, intensified trade wind circulation and cooled surrounding oceans to varying degrees. The cooling of tropics at the LGM would have reduced

humidity levels and rainfall in regions where convergence is important. Moreover, GCMs suggest that the greater relative cooling of the northern hemisphere pushed the austral summer Hadley cell to the south (Clement et al., 2004). The product of these processes was that much of tropical Africa was relatively cool and dry at the LGM, even in the southern hemisphere, despite positive insolation forcing south of the equator (Johnson et al., 2002; Powers et al., 2005; Barker and Gasse, 2003). It is likely that glacial forcing was extremely important throughout the deglaciation, with shifts in the interhemispheric asymmetry altering rainfall patterns.

Cooler SSTs have been estimated for the oceans surrounding southern Africa at the LGM and GCMs using these values generate drier conditions over the region (Pinot et al., 1999). Estimates suggest temperatures in the south-eastern Atlantic fell by up to 3.5 °C (Schneider et al., 1995), whereas those of the south-west Indian Ocean were diminished by only 1.4–2.6 °C (Bard et al., 1997). Under present boundary conditions this zonal

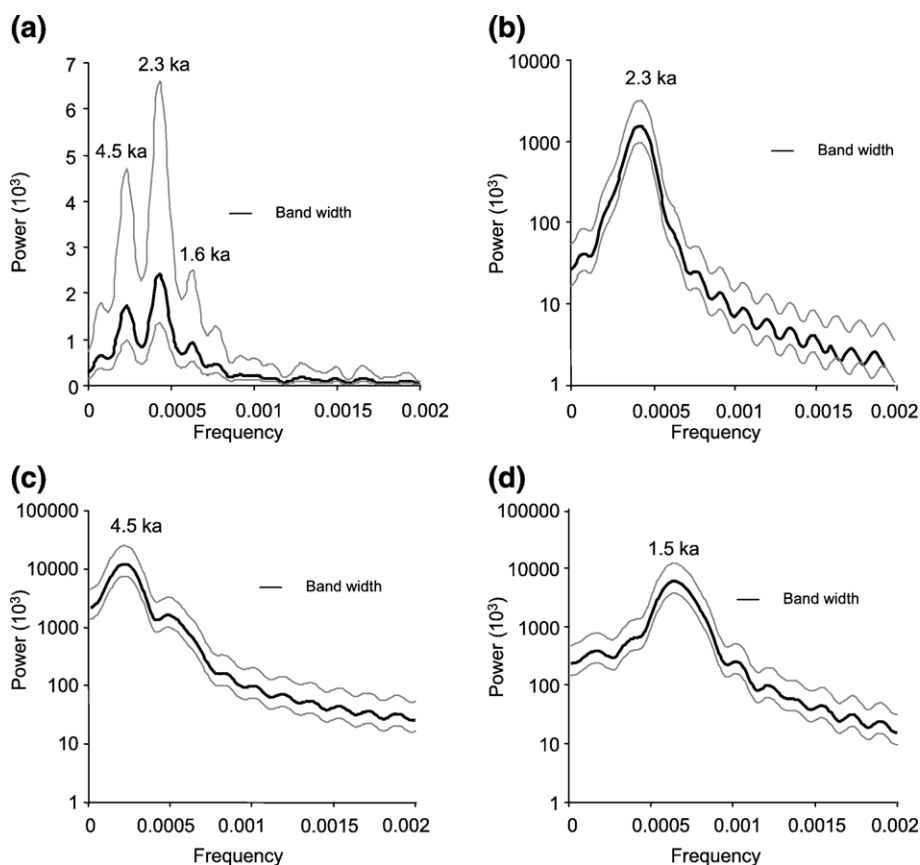


Fig. 5. Blackman–Tukey power spectrum estimation of $\delta^{18}\text{O}_{\text{diatom}}$ data with 80% confidence intervals. (a) Raw $\delta^{18}\text{O}_{\text{diatom}}$, (b) PC 1+2 (41% of variance explained) of SSA filtered $\delta^{18}\text{O}_{\text{diatom}}$ data, (c) PC 3 (14% of variance explained) of SSA filtered $\delta^{18}\text{O}_{\text{diatom}}$ data, (d) PC 5 (7% of variance explained) of SSA filtered $\delta^{18}\text{O}_{\text{diatom}}$ data.

pattern of SSTs arises during El Niño years and creates drier conditions in southern Africa, and less convergence across southern Africa as the main convective zone shifts to the western Indian Ocean. SSTs in the Indian Ocean are a critical control on moisture fluxes to the continent (Goddard and Graham, 1999) and are likely to contribute to the post LGM centennial scale wet–dry intervals revealed by $\delta^{18}\text{O}_{\text{diatom}}$. ENSO forcing would be supported by apparent links across the Indian Ocean to N. Queensland. Here a peat humification record from Lynch's Crater (Turney et al., 2004) thought to result from ENSO processes, reveals a millennial scale structure similar to that of our $\delta^{18}\text{O}_{\text{diatom}}$ record (Fig. 4). For the most part the two records are in-phase, with an exception around 17 ka that may arise from chronological uncertainties.

The structure of our record is comparable to evidence of abrupt events from sites in equatorial East Africa (Gasse, 2000) and processes such as ENSO that presently initiates a rainfall dipole between equatorial and southern Africa must have been largely subservient to meridional mechanisms especially glacial forcing. For example, modelling of a freshwater discharge to the North Atlantic of a magnitude similar to that occurring during the Younger Dryas cool event, produced slightly warmer surface temperatures in the equatorial Atlantic and over the African continent (Dahl et al., 2005). Under this simulation the ITCZ shifted southward and northeasterly trade winds were strengthened. Monsoon winds from the Indian Ocean would also become more northerly, such that reduced convergence occurs and summer rainfall would be diminished (Dahl et al., 2005). In addition, stronger winds from the south during the austral winter would augment evaporation from Lake Malawi as demonstrated by periods of reduced P–E, marked by high $\delta^{18}\text{O}_{\text{diatom}}$ and enhance upwelling and diatom productivity in the northern basin. An alternative ENSO-based explanation of the Younger Dryas has been proposed that involves the Pacific into a La Niña pattern due to orbital configurations (Clement et al., 2001). Using the present as a reference, this scenario would tend to favour wetter conditions in southern Africa, which would be at odds with our data.

These isotope data show strong connections with global climate variability, and it is interesting to observe that quasi-periodicities in the $\delta^{18}\text{O}_{\text{diatom}}$ time series are analogous to periods found in other climate proxies. A dominant periodicity of 2.3 ka yr, broadly describes the spacing of the dry events in this sequence (Fig. 5a). This is exemplified by the first two principle components (PC1+2) generated by the SSA that account for almost 41% of the explained variance (Fig. 5b). We also observe periods at 4.5 ka and less strongly at 1.6 ka in both the

raw and filtered $\delta^{18}\text{O}_{\text{diatom}}$ data. The former is best represented by PC3 (14% of the variance) and the 1.6 ka cycle is mapped by PC 4+5 that cumulatively explain 14% variance (Fig. 5c and d). Similar periods are found in Antarctica at 4.4 ka and 2.4 ka in Vostok temperatures (Yiou et al., 1995), and in Greenland (GISP2) where a 2.3 ka cycle occurs in the K^+ data, and is thought to represent meridional atmospheric circulation (Mayewski et al., 1997). Combination tones and harmonics of orbital cycles have been proposed as mechanisms behind these frequencies (Yiou et al., 1995), as has solar activity (Clemens, 2005). There is less evidence in the time series analysis of direct modulation by thermohaline circulation since, although the relatively weak 1.6 ka cycle is broadly equivalent to North Atlantic rhythms (Bond et al., 2001) given chronological constraints (N. Atlantic is rather 1.47 ka).

Further quantification of the isotope hydrology — climate relationships from these important sites requires extensive calibration of the processes leading to the acquisition and retention of the isotope signal in these new host materials. Nevertheless, the Lake Malawi $\delta^{18}\text{O}_{\text{diatom}}$ record confirms the presence of centennial–millennial scale dry periods in the southern tropics of East Africa since the LGM. We find expressions of the deglaciation driven by re-organisation of SSTs and atmospheric circulation, at a period known from studies of solar variability (Clemens, 2005). Furthermore, abrupt events, well known from the equatorial and northern tropics (Gasse, 2000; Fleitmann et al., 2003) can be observed in this southern hemisphere lake. These isotope data suggest an important role for the tropics in at least amplifying, if not even instigating changes transmitted through Earth's primary atmospheric circulation systems.

Acknowledgements

We wish to thank our partners in the IDEAL project, and especially the co-ordinators Prof T.C. Johnson and Prof. M.R. Talbot, for giving us access to core materials from Lake Malawi and for valuable discussions. Water samples were collected by Mackson Ngochera. Funding for the oxygen isotope analysis was provided by NERC NER/B/S/2002/00512 and IP/800/1103. Hilary Sloane is thanked for conducting the measurement of the diatom oxygen isotope values at NIGL.

References

- Bard, E., 1998. Geochemical and geophysical implications of the radiocarbon calibration. *Geochim. Cosmochim. Acta* 62, 2025–2038.

- Bard, E., Rostek, F., Sonzogni, C., 1997. Interhemispheric synchrony of the last deglaciation inferred from alkenone palaeothermometry. *Nature* 385, 707–710.
- Barker, P.A., Gasse, F., 2003. New evidence for a reduced water balance in East Africa during the Last Glacial Maximum: implication for model–data comparison. *Quat. Sci. Rev.* 22, 823–837.
- Barker, P., Telford, R., Gasse, F., Thevenon, R., 2002. Late Pleistocene and Holocene palaeohydrology of Lake Rukwa, Tanzania, inferred from diatom analysis. *Palaeogeogr. Palaeoclimatol. Palaeoecol.* 187, 295–305.
- Barker, P.A., Talbot, M.R., Street-Perrott, F.A., Marret, F., Scourse, J.D., Odada, E., 2004. Late Quaternary climatic variability in intertropical Africa. In: Battarbee, R.W., Gasse, F., Stickley, C.E. (Eds.), *Past Climate Variability through Europe and Africa. Developments in Palaeoenvironmental Research*. Kluwer Academic Publishers, Dordrecht, pp. 117–138.
- Barry, S.L., Filippi, M.L., Talbot, M.R., Johnson, T.C., 2002. Sedimentology and geochronology of Late Pleistocene and Holocene sediments from northern Lake Malawi. In: Odada, E.O., Olago, D.O. (Eds.), *East African Great Lakes: Limnology, Paleolimnology and Biodiversity, Advances in Global Change Research*. Kluwer Academic Publishers, Dordrecht, pp. 369–391.
- Bergonzini, L., 1998. Bilans hydriques de lacs (Kivu, Tanganyika, Rukwa and Nyassa) du Rift Est Africain. *Musee Royal de L'Afrique Centrale, Tervuren, Belgique*. 183 pp.
- Blunier, T., Brook, E.J., 2001. Timing of millennial-scale climate change in Antarctica and Greenland during the last glacial period. *Science* 291, 109–112.
- Bond, G., Kromer, B., Beer, J., Muscheler, R., Evans, M.N., Showers, W., Hoffmann, S., Lotti-Bond, R., Hajdas, I., Bonani, G., 2001. Persistent solar influence on north Atlantic climate during the Holocene. *Science* 294, 2130–2136.
- Bootsma, H.A., 1993. Spatio-temporal variation of phytoplankton biomass in Lake Malawi, Central Africa. *Verh. - Int. Ver. Theor. Angew. Limnol.* 25, 882–886.
- Bootsma, H.A., Hecky, R.E., Johnson, T.C., Kling, H.J., Mwita, J., 2003. Inputs, outputs, and internal cycling of silica in a large, tropical lake. *J. Great Lakes Res.* 29, 121–138.
- Branchu, P., Bergonzini, L., Delvaux, D., De Batist, M., Golubev, V., Benedetti, M., Klerkx, J., 2005. Tectonic, climatic and hydrothermal control on sedimentation and water chemistry of northern Lake Malawi (Nyasa), Tanzania. *J. Afr. Earth Sci.* 43, 433–446.
- Broecker, W.S., 1998. Paleocirculation during the last deglaciation: a bipolar seesaw? *Paleoceanography* 13, 119–121.
- Brook, E.J., White, J.W.C., Schilla, A.S.M., Bender, M.L., Barnett, B., Severinghaus, J.P., Taylor, K.C., Alley, R.B., Steig, E.J., 2005. Timing of millennial-scale climate change at Siple Dome, West Antarctica, during the last glacial period. *Quat. Sci. Rev.* 24, 1333–1343.
- Chappellaz, J., Blunier, T., Raynaud, D., Barnola, J.M., Schwander, J., Stauffer, B., 1993. Synchronous changes in atmospheric CH_4 and Greenland climate between 40-kyr and 8-kyr bp. *Nature* 366, 443–445.
- Clemens, S.C., 2005. Millennial-band climate spectrum resolved and linked to centennial-scale solar cycles. *Quat. Sci. Rev.* 24, 521–531.
- Clement, A.C., Cane, M.A., Seager, R., 2001. An orbitally driven tropical source for abrupt climate change. *J. Climate* 14, 2369–2375.
- Clement, A.C., Hall, A., Broccoli, A.J., 2004. The importance of precessional signals in the tropical climate. *Clim. Dyn.* 22, 327–341.
- Dahl, K., Broccoli, A., Stouffer, R., 2005. Assessing the role of North Atlantic freshwater forcing in millennial scale climate variability: a tropical Atlantic perspective. *Clim. Dyn.* 24, 325–346.
- Filippi, M.L., Talbot, M.R., 2005. The paleolimnology of northern Lake Malawi over the last 25 ka based upon the elemental and stable isotopic composition of sedimentary organic matter. *Quat. Sci. Rev.* 24, 1303–1328.
- Fleitmann, D., Burns, S.J., Mudelsee, M., Neff, U., Kramers, J., Mangini, A., Matter, A., 2003. Holocene forcing of the Indian monsoon recorded in a stalagmite from Southern Oman. *Science* 300, 1737–1739.
- Gasse, F., 2000. Hydrological changes in the African tropics since the Last Glacial Maximum. *Quat. Sci. Rev.* 19, 189–211.
- Gasse, F., Lédée, V., Massault, M., Fontes, J.C., 1989. Water-level fluctuations of Lake Tanganyika in phase with oceanic changes during the last glaciation and deglaciation. *Nature* 342, 57–59.
- Gasse, F., Barker, P.A., Johnson, T.C., 2002. A 24,000 yr diatom record from the northern basin of Lake Malawi. In: Odada, E.O., Olago, D.O. (Eds.), *East African Great Lakes: Limnology, Paleolimnology and Biodiversity. Advances in Global Change Research*, vol. 12. Kluwer Academic Publishers, Dordrecht, pp. 393–414.
- Ghil, M., Allen, M.R., Dettinger, M.D., Ide, K., Kondrashov, D., Mann, M.E., Robertson, A.W., Saunders, A., Tian, Y., Varadi, F., Yiou, P., 2002. Advanced spectral methods for climatic time series. *Rev. Geophys.* 40 [art. no.-1003].
- Goddard, L., Graham, N.E., 1999. Importance of the Indian Ocean for simulating rainfall anomalies over eastern and southern Africa. *J. Geophys. Res., [Atmos.]* 104, 19099–19116.
- Gonfiantini, R., Zuppi, G.M., Eccles, D.H., Ferro, W., 1979. Isotope investigation of Lake Malawi, isotopes in lake studies. *International Atomic Energy Agency, Vienna*, pp. 195–207.
- Groote, P.M., Stuiver, M., White, J.W.C., Johnsen, S., Jouzel, J., 1993. Comparison of oxygen–isotope records from the GISP2 and GRIP Greenland Ice Cores. *Nature* 366, 552–554.
- Haberyan, K.A., 1987. Fossil diatoms and the paleolimnology of Lake Rukwa, S.W. Tanzania. *Freshw. Biol.* 17, 429–436.
- Hecky, R.E., Kling, H.J., 1987. Phytoplankton ecology of the great lakes in the rift valley of central Africa. *Ergeb. Limnol.* 25, 197–228.
- S.A. Holdship, The paleolimnology of Lake Manyara, Tanzania: a diatom analysis of a 56 meter sediment core, Ph.D. Dissertation, Duke University, 1976.
- Holmgren, K., Lee-Thorp, J.A., Cooper, G.R.J., Lundblad, K., Partridge, T.C., Scott, L., Sthaldeen, R., Talma, A.S., Tyson, P.D., 2003. Persistent millennial-scale climatic variability over the past 25,000 yr in Southern Africa. *Quat. Sci. Rev.* 22, 2311–2326.
- Huang, Y.S., Shuman, B., Wang, Y., Webb, T., 2002. Hydrogen isotope ratios of palmitic acid in lacustrine sediments record Late Quaternary climate variations. *Geology* 30, 1103–1106.
- IAEA/WMO, Global Network for Isotopes in Precipitation. The GNIP Database. Release 3, October 1999. 2000, IAEA/WMO, 1998.
- Johnson, T.C., 1996. Sedimentary processes and signals of past climatic change in the large lakes of the East African Rift valley. In: Johnson, T.C., Odada, E.O. (Eds.), *The Limnology, Climatology and Paleoclimatology of the East African Lakes*. Gordon & Breach, Amsterdam, pp. 367–412.
- Johnson, T.C., Brown, E., McManus, J., Barry, S., Barker, P., Gasse, F., 2002. A high resolution paleoclimate record spanning the past 25,000 yr in southern East Africa. *Science* 296, 113–132.
- Johnson, T.C., Brown, E.T., McManus, J., 2004. Diatom productivity in Northern Lake Malawi during the past 25,000 yr: implications for

- the position of the intertropical convergence zone at millennial and shorter time scales. In: Battarbee, R.W., Gasse, F., Stickley, C.E. (Eds.), *Past Climate Variability through Europe and Africa*. Developments in Paleoenvironmental Research, vol. 6. Springer, Dordrecht, pp. 93–116.
- Jouzel, J., Vaikmaa, R., Petit, J.R., Martin, M., Duclos, Y., Stievenard, M., Lorius, C., Toots, M., Melieres, M.A., Burckle, L.H., Barkov, N.I., Kotlyakov, V.M., 1995. The 2-step shape and timing of the last deglaciation in Antarctica. *Clim. Dyn.* 11, 151–161.
- Juillet-Leclerc, A., Labeyrie, L., 1987. Temperature dependence of the oxygen isotopic fractionation between diatom silica and water. *Earth Planet. Sci. Lett.* 84, 69–74.
- Jury, M.R., Mpeta, E.J., 2004. The annual cycle of African climate and its variability. *Water South Africa* 31, 1–8.
- Jury, M.R., Mwafurirwa, N.D., 2002. Climate variability in Malawi, part 1: dry summers, statistical associations and predictability. *Int. J. Climatol.* 22, 1289–1302.
- Leng, M.J., Barker, P.A., 2006. A review of the oxygen isotope composition of diatom silica for palaeoclimate reconstruction. *Earth Sci. Rev.* 75, 5–27.
- Mayewski, P.A., Meeker, L.D., Twickler, M.S., Whitlow, S., Yang, Q.Z., Lyons, W.B., Prentice, M., 1997. Major features and forcing of high-latitude northern hemisphere atmospheric circulation using a 110,000-year-long glaciochemical series. *J. Geophys. Res., [Oceans]* 102, 26345–26366.
- McHugh, M.J., Rogers, J.C., 2001. North Atlantic oscillation influence on precipitation variability around the southeast African convergence zone. *J. Climate* 14, 3631–3642.
- Meehl, G.A., van Loon, H., 1979. The seesaw in winter temperatures between Greenland and Northern Europe. Part III. Teleconnections with Lower Latitudes. *Mon. Weather Rev.* vol. 107, 1095–1106.
- Nicholson, S.E., 1997. An analysis of the ENSO signal in the tropical Atlantic and western Indian Oceans. *Int. J. Climatol.* 17, 345–375.
- Oerter, H., Graf, W., Meyer, H., Wilhelms, F., The EPICA ice core from Dronning Maud Land: first results from stable-isotope measurements, *Annals of Glaciology*, Vol 39, 2005, *Annals of Glaciology* 39, 2004, pp. 307–312.
- Paillard, D., Labeyrie, L., Yiou, P., 1996. Macintosh program performs time-series analysis. *EOS, Trans. - Am. Geophys. Union* 77.
- Pinot, S., Ramstein, G., Harrison, S.P., Prentice, I.C., Guiot, J., Stute, M., Joussaume, S., 1999. Tropical paleoclimates at the Last Glacial Maximum: comparison of Paleoclimate Modeling Intercomparison Project (PMIP) simulations and paleodata. *Clim. Dyn.* 15, 857–874.
- Powers, L.A., Johnson, T.C., Werne, J.P., Castañeda, I.S., 2005. Large temperature variability in the southern African tropics since the Last Glacial Maximum. *Geophys. Res. Lett.* 32. doi:10.1029/2004GL022014.
- Ricketts, R.D., 1998. A comparison between the stable isotope composition of Early Holocene and Late Pleistocene carbonates from Lake Malawi, East Africa. In: Lehman, J.T. (Ed.), *Environmental Change and Response in East African Lakes*. Monographiae Biologicae, vol. 79. Kluwer, pp. 191–206.
- Roberts, N., Taieb, M., Barker, P., Damnati, B., Icole, M., Williamson, D., 1993. Timing of the Younger Dryas event in East Africa from lake-level changes. *Nature* 366, 146–148.
- Rosenthal, Y., Broccoli, A.J., 2004. In search of paleo-ENSO. *Science* 304, 219–221.
- Rozanski, K., Araguas-Araguas, L., Gonfiantini, R., 1996. Isotope patterns of precipitation in the East Africa region. In: Johnson, T.C., Odada, E.O. (Eds.), *The Limnology, Climatology and Paleoclimatology of the East African lakes*. Gordon & Breach, Amsterdam, pp. 79–93.
- Russell, J.M., 2004. The Holocene Paleolimnology and Paleoclimatology of Lake Edward, Uganda-Congo University of Minnesota.
- Sachse, D., Radke, J., Gleixner, G., 2004. Hydrogen isotope ratios of recent lacustrine sedimentary *n*-alkanes record modern climate variability. *Geochim. Cosmochim. Acta* 68, 4877–4889.
- Schmidt, M., Botz, R., Rickert, D., Bohrmann, G., Hall, S.R., Mann, S., 2001. Oxygen isotopes of marine diatoms and relations to opal-A maturation. *Geochim. Cosmochim. Acta* 65, 201–211.
- Schneider, R., Müller, P.J., Ruhland, G., 1995. Late Quaternary surface circulation in the eastern equatorial South Atlantic: evidence from alkenone sea surface temperature. *Paleoceanography* 10, 197–219.
- Shemesh, A., Charles, C.D., Fairbanks, R.G., 1992. Oxygen isotopes in biogenic silica — global changes in ocean temperature and isotopic composition. *Science* 256, 1434–1436.
- Stocker, T.F., 1998. Climate change — the seesaw effect. *Science* 282, 61–62.
- Stott, L., Poulsen, C., Lund, S., Thunell, R., 2002. Super ENSO and global climate oscillations at millennial time scales. *Science* 297, 222–226.
- Stuiver, M., Reimer, P.J., Bard, E., Beck, J.W., Burr, G.S., Hughen, K.A., Kromer, B., McCormac, F.G., van der Plicht, J., Spurk, M., 1998. Radiocarbon Calibration Program REV 4.0/CALIB 4.0. *Radiocarbon* 40, 1041–1083.
- Turney, C.S.M., Kershaw, A.P., Clemens, S.C., Branch, N., Moss, P.T., Fifield, L.K., 2004. Millennial and orbital variations of El Nino/Southern Oscillation and high-latitude climate in the last glacial period. *Nature* 428, 306–310.
- Yiou, P., Jouzel, J., Johnsen, S., Rognvaldsson, O.E., 1995. Rapid oscillations in Vostok and Grip Ice cores. *Geophys. Res. Lett.* 22, 2179–2182.